

Bead on a rotating circular hoop: a simple yet feature-rich dynamical system

Shovan Dutta¹ and Subhankar Ray²

¹ *Department of Electronics and Telecommunication Engineering,*

Jadavpur University, Calcutta 700 032, India and

² *Department of Physics, Jadavpur University, Calcutta 700 032, India*

The motion of a bead on a rotating circular hoop is investigated using elementary calculus and simple symmetry arguments. The peculiar trajectories of the bead at different speeds of rotation of the hoop are presented. Phase portraits and nature of fixed points are studied. Bifurcation is observed with change in the rotational speed of the hoop. At a critical speed of rotation of the hoop, there appears an interesting relation between the time period and amplitude of oscillation of the bead. The study introduces several important aspects of nonlinear dynamics. It is suitable for students having basic understanding in elementary calculus and classical mechanics.

PACS numbers: 05.45.-a, 45.20.dg, 03.65.Ge, 11.30.Qc

I. INTRODUCTION

A bead moving on a rotating circular hoop is a classic example studied in several textbooks on classical mechanics^{1–3} and nonlinear dynamics. It exhibits various modes of motion, including some peculiar ones, such as, oscillations confined to one side of the hoop and complete revolutions, for appropriate initial conditions. It also shows a wide array of features of dynamical systems. It is useful for demonstrating different classes of fixed points, bifurcations, reversibility, symmetry breaking, critical slowing down, trapping regions, homoclinic and heteroclinic orbits and Lyapunov functions. It is also an interesting example of a constrained system, illustrating the use of Lagrange multipliers for determining constraint forces.

In this article we investigate in detail, the dynamics of this bead-hoop system. The number and nature of equilibrium points alter with change in speed of rotation of the hoop. This results in some extraordinary modes of motion, phase trajectories and bifurcations. At a critical speed of rotation of the hoop, an interesting relation between the time period and amplitude of oscillation of the bead is observed.

Our study is based on elementary calculus and simple symmetry arguments. A student reader with a background of classical mechanics and basic calculus will find the study both accessible and interesting.

The article is organized as follows. In section II, the physical system is described. The equation of motion of the system is derived from the Lagrangian. In section III, the effective potential is analyzed to find the equilibrium positions of the bead for all possible speeds of rotation of the hoop. The distinct modes of motion of the bead for different initial conditions are described and numerical plots of its trajectories are presented. The constraint forces are determined from the method of Lagrange multipliers in section IV. In section V, the nature of the fixed points of the system are analyzed from symmetry properties of the system. The phase trajectories and bifurcations are examined. Finally, we conclude with a discussion on connections to other systems in section VI.

II. THE PHYSICAL SYSTEM

A bead of mass m , moves without friction on a circular hoop of radius a . The hoop rotates about its vertical diameter with a constant angular velocity ω . The position of the bead on the hoop is given by angle θ , measured from the vertically downward direction ($-z$ axis), and ϕ is the angular displacement of the hoop from its initial position on the x -axis (Figure 1).

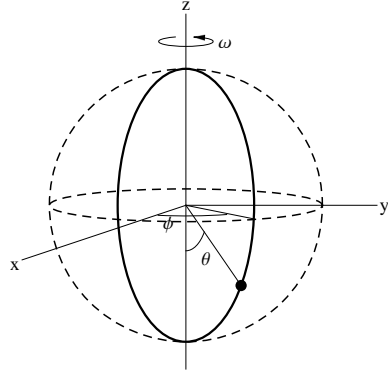


FIG. 1. Schematic diagram for bead on the hoop

The kinetic and potential energies of the bead are given by,

$$T = \frac{1}{2}ma^2(\dot{\theta}^2 + \sin^2 \theta \dot{\phi}^2) \quad \text{and} \quad V = -mga \cos \theta, \quad (1)$$

respectively, where g is the magnitude of the acceleration due to gravity. The Lagrangian of the system is,

$$L(\theta, \dot{\theta}) = \frac{ma^2}{2}(\dot{\theta}^2 + \omega^2 \sin^2 \theta) + mga \cos \theta, \quad \text{where } \omega = \dot{\phi} \text{ (a constant).} \quad (2)$$

Using the Euler-Lagrange equation, the equation of motion is obtained as,

$$\ddot{\theta} = \sin \theta (\omega^2 \cos \theta - g/a). \quad (3)$$

Denoting $\omega_c^2 = g/a$, $k = \omega^2/\omega_c^2$ and defining $\tau = \omega_c t$, the equation of motion may be written in dimensionless form as,

$$\theta'' = \sin \theta (k \cos \theta - 1), \quad \text{where } \theta'' = \frac{d^2\theta}{d\tau^2}. \quad (4)$$

The symmetry of the system about the vertical axis manifests in the invariance of the equation of motion when θ is changed to $-\theta$. The system also exhibits time reversal symmetry as (4) is invariant under the transformation $\tau \rightarrow -\tau$.

Let us denote $v = \theta'$ and write (4) as,

$$v \frac{dv}{d\theta} = -\sin \theta + k \sin \theta \cos \theta, \quad (5)$$

which upon integration yields,

$$\frac{1}{2}v^2 = \cos \theta - \frac{k}{4} \cos 2\theta + A, \quad (6)$$

where A is a constant of integration. We can identify a conserved quantity, ε as,

$$\varepsilon = \frac{1}{2}\theta'^2 - \frac{1}{2}k \sin^2 \theta - \cos \theta. \quad (7)$$

It may be termed as the effective energy that corresponds to the system described by (4). However, it is to be noted that, the mechanical energy of the original bead-hoop system is not conserved due to the work done in preserving the constant angular velocity of the hoop. Equation (7) provides a natural separation of the effective energy into effective kinetic energy $\frac{1}{2}\theta'^2$ and effective potential energy, $U(\theta)$, given by,

$$U(\theta) = -\frac{1}{2}k \sin^2 \theta - \cos \theta. \quad (8)$$

As $U(\theta)$ is an even function of θ , we restrict our attention to $\theta \in [0, \pi]$. θ'^2 is completely determined by θ and ε . The sign of θ' , however, cannot be determined uniquely from (7). The parameter k grows with increasing angular velocity ω of the hoop and $k = 0$ implies that the hoop is stationary.

It is useful to consider the first and second derivatives of $U(\theta)$,

$$U'(\theta) = \frac{dU}{d\theta} = -\sin \theta(k \cos \theta - 1), \quad \text{and} \quad (9)$$

$$U''(\theta) = \frac{d^2U}{d\theta^2} = -(k \cos 2\theta - \cos \theta). \quad (10)$$

Comparison of (4) and (9) shows that,

$$\theta'' = -U'(\theta) = -\sin \theta(1 - k \cos \theta). \quad (11)$$

The effective potential has two extrema at $\theta = 0$ and $\theta = \pi$, where the first derivative of the potential vanishes. Evaluating the second derivative at these points, one finds that $\theta = 0$ is a minimum ($U''(0) > 0$) and $\theta = \pi$ is a maximum ($U''(0) < 0$) of the effective potential as shown in Figure 2. Due to the right-left symmetry of the hoop, one concludes, $\theta = -\pi$ is also a maximum point of the effective potential. At these points the values of the effective potential are $U(0) = U_{min} = -1$ and $U(\pm\pi) = U_{max} = 1$.

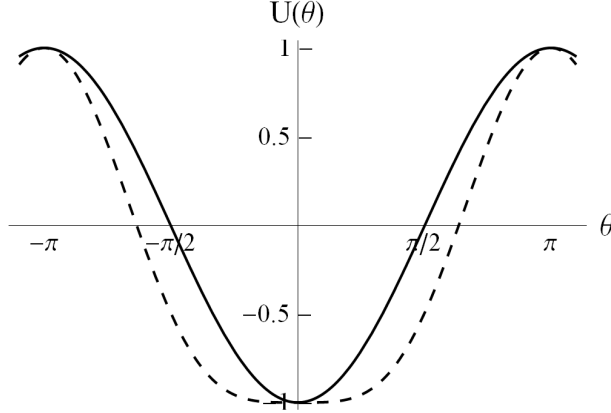


FIG. 2. Minimum of $U(\theta)$ is flatter and maxima sharper as $k \rightarrow 1$. The solid curve is for $k = 0.010$, dashed curve is for $k = 0.998$

III. MODES OF MOTION AND TRAJECTORIES OF THE BEAD

A. $0 \leq k < 1$

When $k = 0$, the effective potential takes the form of the potential energy of a pendulum. As k increases from zero towards 1, $U''(0) \rightarrow 0$ and $|U''(\pm\pi)| \rightarrow 2$, implying that the minimum at $\theta = 0$ is flatter and the maxima at $\theta = \pm\pi$ are sharper (Figure 2).

For $k \neq 0$, at different effective energy values, the actual motion of the bead will depend on the initial conditions which we discuss below.

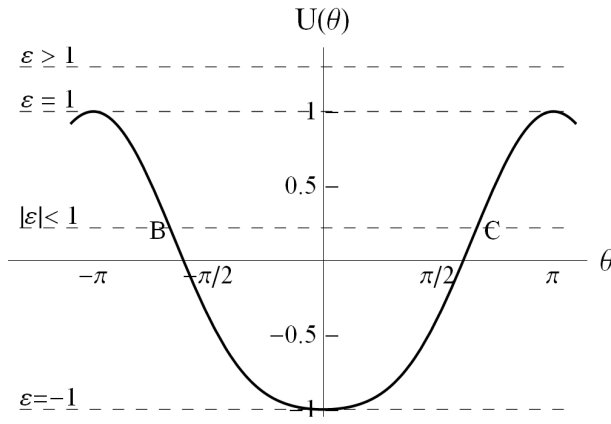


FIG. 3. Effective potential $U(\theta)$ versus θ for $0 \leq k < 1$

(i) Effective energy, $\varepsilon = -1$

$\theta'^2 = 2(\varepsilon - U(\theta))$ must be positive, hence the lower bound of ε is equal to the minimum value of $U(\theta)$ which is -1 (Figure 3). This corresponds to the initial condition $\theta(0) = 0$ and $\theta'(0) = 0$. From (11) however, $\theta'' = 0$ as well, independent of the value of k . Hence, the bead stays at the bottom of the hoop ($\theta = 0$) for all times.

(ii) $-1 < \varepsilon < 1$

The angular position θ of the bead oscillates between $-\theta_0$ and $+\theta_0$, corresponding to the turning points B and C shown in Figure 3. At these points $\theta' = 0$, and the effective potential equals the effective energy. From (4), $\theta'' < 0$ and this restoring acceleration ensures that θ

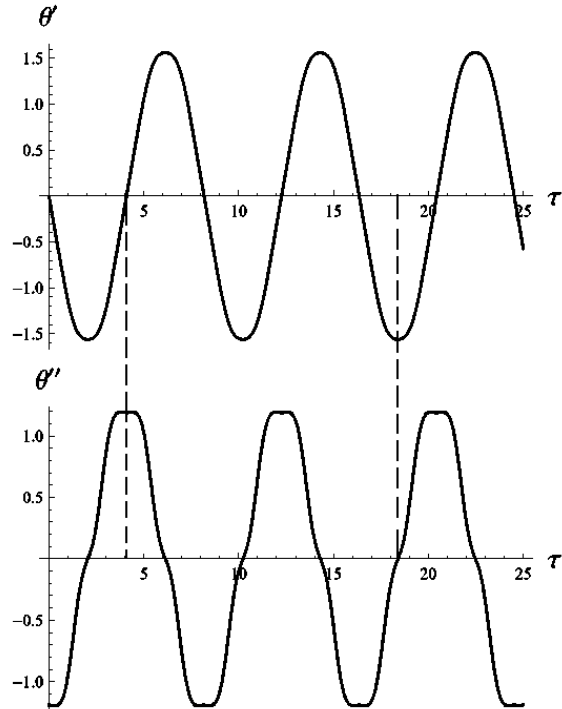


FIG. 4. Out of phase oscillation of θ' and θ'' for $k = 0.75$, $\theta_0 = 2\pi/3$

approaches 0. At $\theta = 0$, acceleration θ'' is zero, whereas the velocity θ' attains its maximum magnitude. Hence, the bead slides past the bottom of the hoop and θ decreases further, becoming negative. When $\theta < 0$, θ'' becomes positive, and this acceleration reduces the magnitude of θ' , making it zero at $-\theta_0$. θ'' remains nonzero and positive at $-\theta_0$. The acceleration θ'' is positive for all negative values of θ . At $\theta = -\theta_0$, $\theta'' > 0$ and velocity is momentarily zero. From the next instant, velocity begins to increase as $\theta'' > 0$. Thus θ' and

θ'' oscillate out of phase with each other as shown in Figure 4. At $-\theta_0$, $\theta'' > 0$, θ' becomes positive, θ begins to increase. The bead retraces its path reaching θ_0 and the process is repeated. The amplitude of oscillation increases with ε . The time period of the oscillation of the bead between $\pm\theta_0$ is given by,

$$T = 4 \int_0^{\theta_0} \frac{d\theta}{\sqrt{(\cos \theta - \cos \theta_0)(2 - k(\cos \theta + \cos \theta_0))}} . \quad (12)$$

Figure 5 shows the trajectory of the bead after the elapse of different time intervals, with $k = 3/4$ and amplitude $\theta_0 = 2\pi/3$. As the bead goes through half an oscillation (with amplitude $2\pi/3$ and $k = 3/4$), the hoop rotates through an angle given by,

$$\Delta\phi = \omega \left(\sqrt{\frac{a}{g}} \frac{T}{2} \right) = \frac{\sqrt{k}}{2} T = 3.539 \text{ radians} .$$

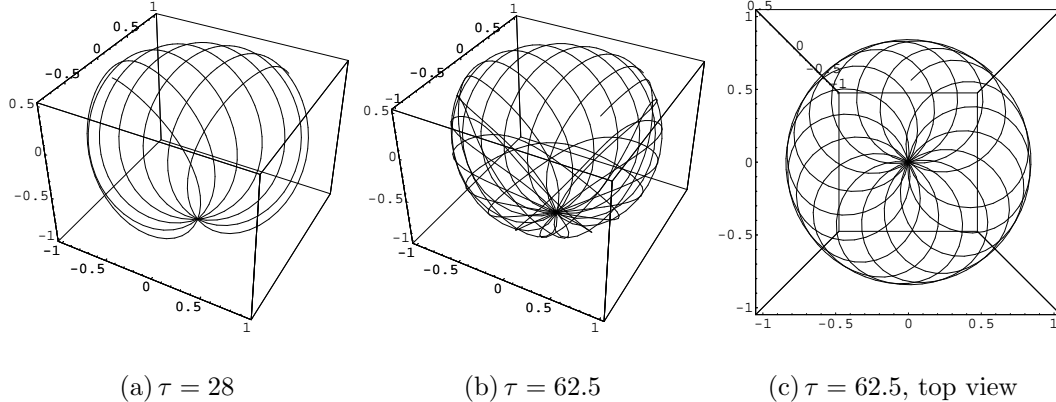


FIG. 5. Trajectory for $k=0.75$, $\theta(0) = 2\pi/3$, $\theta'(0) = 0$ at different τ values

(iii) $\varepsilon = 1$

At $\theta = \pm\pi$, the effective potential energy is also $+1$. Thus the effective kinetic energy and θ' is zero. From the expression of acceleration in (4), we find $\theta'' = 0$ at $\theta = \pm\pi$. This agrees with the fact that $\theta = \pm\pi$ are the position of maximum potential energy. From (7), we obtain,

$$\theta'^2 = 4 \cos^2 \frac{\theta}{2} [1 + k \sin^2 \frac{\theta}{2}] . \quad (13)$$

The time taken to reach the highest point ($\theta = \pi$) from an initial point θ_0 may be computed as,

$$T = \frac{1}{2} \int_{\theta_0}^{\pi} \frac{d\theta}{\cos(\theta/2) \sqrt{1 + k \sin^2(\theta/2)}} \quad (14)$$

The integral can be transformed with the substitution $u = \pi - \theta$, as,

$$T = \frac{1}{2} \int_0^{\pi-\theta_0} \frac{du}{\sin(u/2) \sqrt{1 + k \cos^2(u/2)}} \quad (15)$$

In the neighbourhood of $u = 0$, corresponding to θ close to π , the integrand behaves as $\frac{(1+k)^{-1/2}}{u}$ and hence, the integral diverges. This implies that the bead approaches $\theta = \pi$ infinitesimally slowly and takes an infinite amount of time to reach the top of the hoop (Figure 6). By virtue of time-reversal symmetry and the left-right symmetry of the hoop,

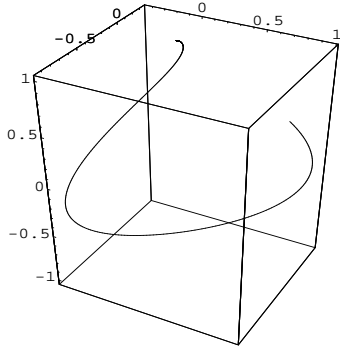


FIG. 6. Trajectory for $k = 0.75$, $\theta(0) = 2\pi/3$ and $\varepsilon = 1$

for $\theta'(0) < 0$, the bead reaches the bottom where θ' has the maximum magnitude of 2 (from (7)) and then asymptotically approaches $\theta = -\pi$ at ever-decreasing speed.

(iv) $\varepsilon > 1$

As the maximum value of $U(\theta) = 1$, $\varepsilon - U(\theta) > 0$ and hence θ' is not zero for any θ . Thus if the bead starts initially with $\theta'(0) > 0$ and at a position $\theta(0) \in (0, \pi)$, then $\theta''(0) < 0$ and θ' starts to decrease. θ' attains its minimum value when the bead reaches $\theta = \pi$. At this position, $\theta'' = 0$, however, θ' is not zero and θ continues to increase. Hence the bead moves past the top of the loop. For $\theta \in (\pi, \frac{3\pi}{2})$, θ'' is positive and θ' increases, becoming maximum when the bead reaches the bottom of the hoop. Thus θ increases or decreases indefinitely, depending on the sign of $\theta'(0)$ and the bead slides over the entire hoop periodically (Figure 7). For $\theta'(0) < 0$, the same rotation occurs in the opposite sense. The maximum and minimum values of θ' can be calculated from the expression of the effective energy. The time period of rotation is given by,

$$T = 2 \int_0^\pi \frac{d\theta}{\sqrt{(\theta'(0))^2 - (\cos \theta - \cos \theta_0)[2 - k(\cos \theta + \cos \theta_0)]}} \quad (16)$$

When $|\theta'(0)|$ is very large, nearly all the energy of the bead is the kinetic energy of rotation. Hence the influence of gravity becomes small in comparison, and this rotation may be considered to be uniform. In this limit, the time period approaches the value $2\pi/|\theta'(0)|$.

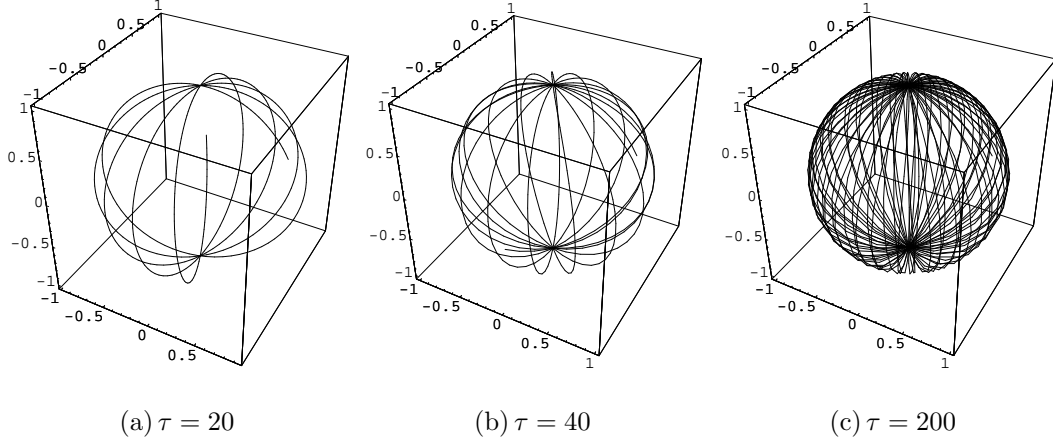


FIG. 7. Trajectory for $k=0.01$, $\theta(0) = 2\pi/3$, $\theta'(0) = 1.4$ for different τ .

B. $k = 1$

$U(\theta)$ is maximum at $\theta = \pi$ as before. However, at $\theta = 0$, both $U'(0)$ and $U''(0)$ vanish. On expanding $U(\theta)$ about $\theta = 0$, we get,

$$U(\theta) = -1 + \frac{\theta^4}{8} + O(\theta^6).$$

For $|\theta| \geq 0$, in the neighbourhood of $\theta = 0$, $U(\theta)$ is always greater than $U(0)$. Hence $\theta = 0$ is a minimum of the potential. The potential is more flat than for the case $k < 1$. Depending on the values of ε , the bead can undergo all the types of motion described in the previous subsection. However, for oscillatory motion, the period of oscillation for a given amplitude is larger when $k = 1$ than when $k < 1$. This becomes clear if (4) is expanded in the vicinity of $\theta = 0$,

$$\begin{aligned} \theta'' &= (\theta - \frac{\theta^3}{3!} + \dots)[k(1 - \frac{\theta^2}{2!} + \dots) - 1] \\ &= -(1 - k)\theta - \left(\frac{2k}{3} - \frac{1}{6}\right)\theta^3 + O(\theta^5) \end{aligned}$$

When $k < 1$, $\theta'' \sim O(\theta)$, however, for $k = 1$, $\theta'' \sim O(\theta^3)$. For small amplitude θ ($\theta \rightarrow 0$), $\theta''_{k=1}(\sim O(\theta^3))$ is much smaller than $\theta''_{k<1}(\sim O(\theta))$. Thus θ' changes much more slowly in the

neighbourhood of $\theta = 0$ for $k = 1$. Consequently, the period of oscillation T , for the same amplitude is significantly larger.

TABLE I. Time period of oscillations for different amplitudes at various k values.

T about $\theta = 0$	$k = 0$	$k = 0.5$	$k = 0.75$	$k = 1$
amplitude $\pi/10$	6.32	8.78	12.00	33.71
amplitude $= \pi/20$	6.29	8.86	12.41	66.93
amplitude $= \pi/40$	6.29	8.88	12.53	133.62
amplitude $= \pi/80$	6.28	8.88	12.55	267.12

Table I lists the time periods computed for different amplitudes at various values of k . The values in the table reveal a very interesting pattern. For small amplitudes, the time period is essentially independent of amplitude when $0 \leq k < 1$; but for $k = 1$, the time period increases inversely as the decrease in amplitude. This is explained as follows. For $0 \leq k < 1$, the effective potential is approximately parabolic in the neighbourhood of $\theta = 0$, analogous to the simple pendulum. Thus, the small amplitude motion of the bead is simple harmonic, for which the time period is independent of amplitude. However, this parabolic approximation does not hold when $k = 1$, as the second derivative of the effective potential, $U''(\theta)$, vanishes at $\theta = 0$. Using (12), the time period of oscillation for $k = 1$ can be calculated as follows,

$$T = 4 \int_0^{\theta_0} \frac{d\theta}{\sqrt{(\cos \theta - \cos \theta_0)(2 - \cos \theta - \cos \theta_0)}}. \quad (17)$$

Expanding the integrand for small θ_0 gives,

$$T = 4 \int_0^{\theta_0} \frac{d\theta}{\sqrt{\left(\frac{\theta_0^2 - \theta^2}{2!} - \frac{\theta_0^4 - \theta^4}{4!} + \frac{\theta_0^6 - \theta^6}{6!} + \dots\right) \left(\frac{\theta_0^2 + \theta^2}{2!} - \frac{\theta_0^4 + \theta^4}{4!} + \frac{\theta_0^6 + \theta^6}{6!} + \dots\right)}}$$

Retaining terms up to eighth order in θ_0 ,

$$\begin{aligned} T &= 4 \int_0^{\theta_0} \frac{d\theta}{\sqrt{\frac{1}{4}(\theta_0^4 - \theta^4) - \frac{1}{24}(\theta_0^6 - \theta^6) + \frac{1}{320}(\theta_0^8 - \theta^8)}} \\ &= \frac{8}{\theta_0^2} \int_0^{\theta_0} \frac{d\theta}{\sqrt{1 - \left(\frac{\theta}{\theta_0}\right)^4 - \frac{\theta_0^2}{6}\left(1 - \left(\frac{\theta}{\theta_0}\right)^6\right) + \frac{\theta_0^4}{80}\left(1 - \left(\frac{\theta}{\theta_0}\right)^8\right)}} \end{aligned}$$

Defining a new variable $y = \theta/\theta_0$, this can be expressed as,

$$\begin{aligned} T &= \frac{8}{\theta_0} \int_0^1 \frac{dy}{\sqrt{1 - y^4 - \frac{\theta_0^2}{6}(1 - y^6) + \frac{\theta_0^4}{80}(1 - y^8)}} \\ &= \frac{8}{\theta_0} \int_0^1 \frac{dy}{\sqrt{1 - y^4}} \left[1 - \frac{\theta_0^2}{6} \frac{1 - y^6}{1 - y^4} + \frac{\theta_0^4}{80} \frac{1 - y^8}{1 - y^4} \right]^{-1/2} \end{aligned}$$

Expanding the quantity within brackets in a binomial series and retaining terms upto fourth order in θ_0 ,

$$T = \frac{A}{\theta_0} + B\theta_0 + C\theta_0^3 + O(\theta_0^5) \quad (18)$$

where the constants are given by,

$$A = 8 \int_0^1 \frac{dy}{\sqrt{1 - y^4}} = 10.49 \quad (19)$$

$$B = \frac{2}{3} \int_0^1 \frac{1 - y^6}{(1 - y^4)^{3/2}} dy = 1.04 \quad (20)$$

$$C = \int_0^1 \left(\frac{1}{12} \frac{(1 - y^6)^2}{(1 - y^4)^{5/2}} - \frac{1}{20} \frac{1 - y^8}{(1 - y^4)^{3/2}} \right) dy = 0.07 \quad (21)$$

This shows that for small θ_0 , $T \approx A/\theta_0$, which explains why T doubles when the amplitude is halved. Equation (18) gives a very good approximation even if θ_0 is not close to 0, e.g., for $\theta_0 = \pi/2$, the error is only -0.58% (Figure 8). This can be accounted for by noting that the coefficients of higher order terms in θ_0 decrease rapidly. Thus the expansion converges very fast. As an example, for $\theta_0 = 1$, the third term in (18) contributes only about 0.67% of the first term. Another point to be noted is that the time period of oscillation for $k = 0$, increases with amplitude, whereas, for higher values of k ($k > 0.3$), the time period decreases initially with amplitude (Fig 9). As Eventually for all k , the time period approaches ∞ as the amplitude approaches π .

C. $\mathbf{k} > 1$

When $k > 1$, in addition to $\theta = 0$ and $\theta = \pi$, a new extremum of the potential appears at $\Omega_1 = \cos^{-1}(1/k)$. From (10), it may be shown,

$$U''(0) = -(k - 1) < 0, \quad U''(\pi) = -(k + 1) < 0, \quad U''(\Omega_1) = \left(k - \frac{1}{k} \right) > 0. \quad (22)$$

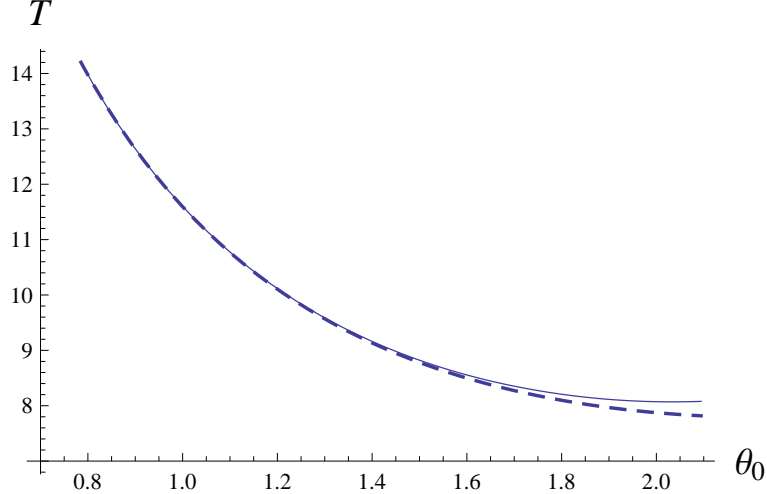


FIG. 8. Time period vs amplitude: solid curve represents accurate plot given by (17), dashed curve represents approximate plot given by (18)

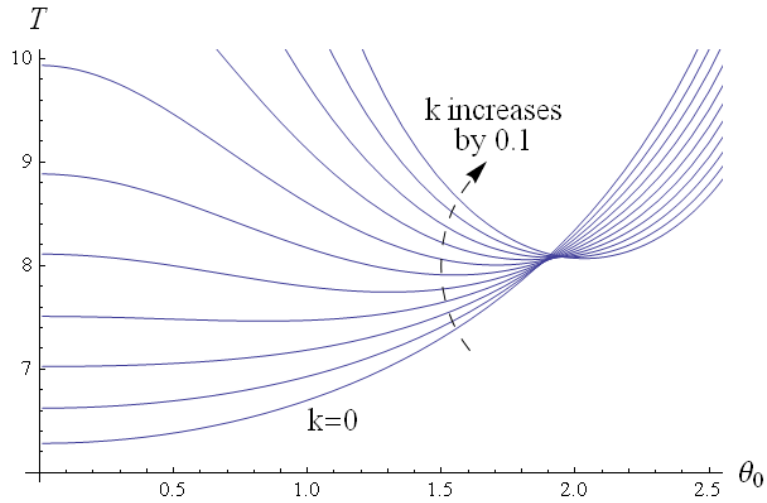


FIG. 9. Variation of time period with amplitude at various values of k

$\theta = \pi$ remains a maximum of the effective potential, however, $\theta = 0$ which was a minimum for $k \leq 1$, is now a maximum. The minimum is at $\theta = \Omega_1$, where,

$$U(\Omega_1) = -\frac{1}{2} \left(k + \frac{1}{k} \right).$$

The effective potential is now a double well as shown in Figure 10. Due to left-right symmetry of the hoop, $-\Omega_1$ is also a minimum of the potential. For $k > 1$, the potential value at Ω_1 is less than -1 , and the value decreases monotonically as k increases. So, the minimum at $\theta = \Omega_1$ becomes deeper with increase in k . As k increases from 1 towards ∞ , Ω_1 increases

from 0 to $\pi/2$ in a monotonic manner. The maximum at $\theta = 0$ is less than the maximum at $\theta = \pi$.

As in the previous section, the motion of the bead in different effective energy regions can

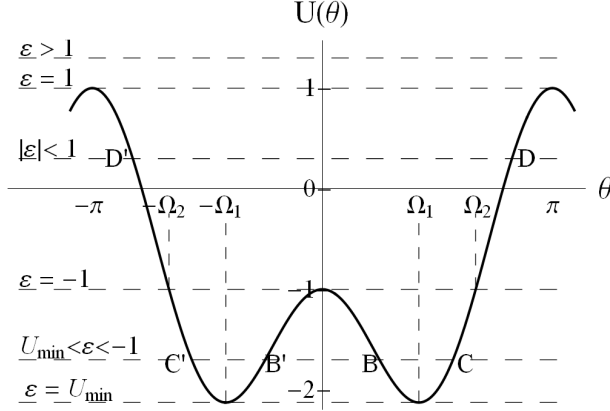


FIG. 10. Effective potential $U(\theta)$ versus θ for $k > 1$.

be identified as follows.

(i) $\varepsilon = -1/2(k + 1/k)$:

The only two possible positions of the bead are at $\pm\Omega_1$, where both θ' and θ'' are zero. Here, even though the minima of the effective potential are symmetric; depending on the initial conditions, one or the other of these minima will be chosen, leading to a breaking of symmetry⁴. As the hoop rotates about its vertical axis, the bead simply moves on a circle of radius $a \sin \Omega_1$.

(ii) $-1/2(k + 1/k) < \varepsilon < -1$:

The bead oscillates between $\theta = \pm\alpha$ to $\theta = \pm\beta$ corresponding to the turning points B, C about Ω_1 , or B', C' about $-\Omega_1$. This is similar to the oscillations encountered for the cases $0 \leq k < 1$ and $k = 1$, except that, here, the oscillations are confined to one side of the hoop (with respect to the vertical axis) and are not symmetric about the minima $\pm\Omega_1$. The bead swings for longer time below the equilibrium point than above it. As $\theta' = 0$ at α and β , we may write using (7),

$$\begin{aligned} \cos \alpha + \cos \beta &= 2 \cos \Omega_1 \quad \text{or,} \\ \cos \frac{\alpha + \beta}{2} \cos \frac{\alpha - \beta}{2} &= \cos \Omega_1 \end{aligned}$$

Hence, $\cos \frac{\alpha + \beta}{2} > \cos \Omega_1$ or, $\Omega_1 - \alpha > \beta - \Omega_1$. Thus the turning point B in Figure 10 is

farther from the point of equilibrium Ω_1 , than the other turning point C . The shape of the effective potential also confirms this (see Figures 10 and 11). About $\theta = 0$, the potential is symmetric, whereas, about $\theta = \Omega_1$, it has a steeper ascent towards π than toward 0. This asymmetry in the shape of the potential decreases as k assumes larger values (Figure 11). This is illustrated in Figure 11 where this asymmetry is shown for $\theta > 0$. In Figure 12, the variation of the potential energy of the bead as it oscillates about Ω_1 is shown with $\alpha \approx \Omega_1 - 60^\circ$. R is the ratio of the time spent below the equilibrium position Ω_1 , to the time spent above it. The period of oscillation can be computed as,

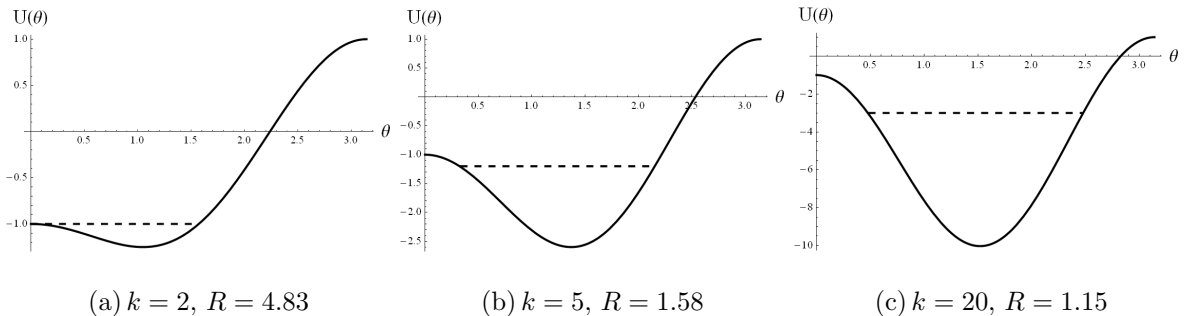


FIG. 11. Asymmetry in the effective potential about its minimum Ω_1 at different k values for $\theta > 0$.

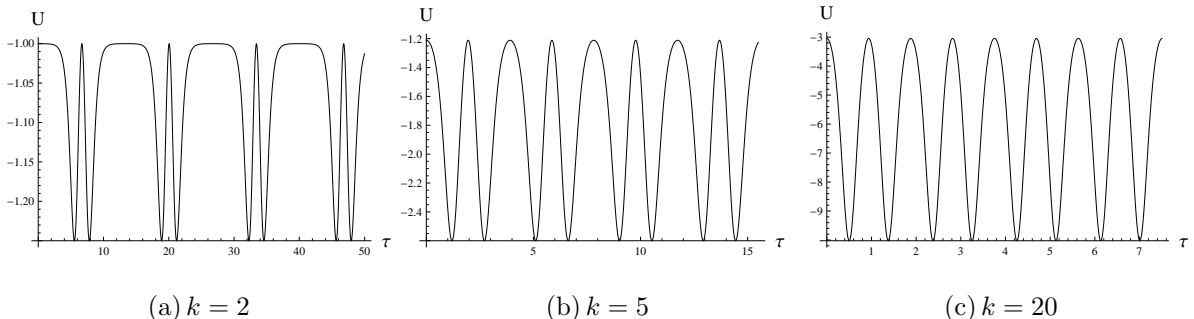


FIG. 12. Change in the potential energy of the bead with time at different k values.

$$T = \frac{2}{\sqrt{k}} \int_{\alpha}^{\beta} \frac{d\theta}{\sqrt{(\cos \alpha - \cos \theta)(\cos \theta - \cos \beta)}} \quad (23)$$

The trajectory of the bead is confined within a band from $\theta = \alpha$ to $\theta = \beta$, on the surface of a sphere of radius a (Figure 13).

(iii) $\varepsilon = -1$:

The motion of the bead is confined within $\theta = 0$ and a certain Ω_2 , where θ' is zero and U

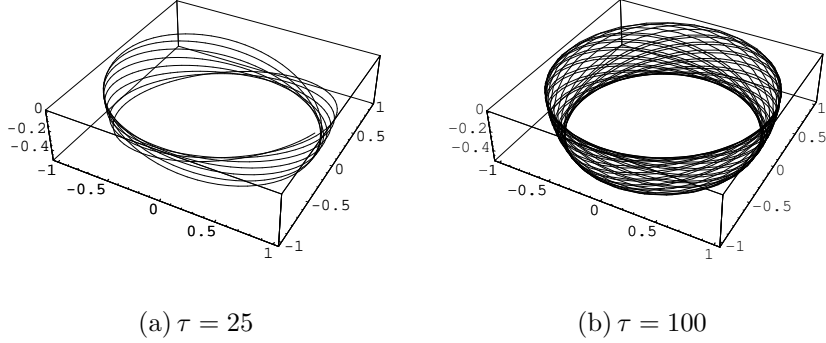


FIG. 13. Trajectory for $k=4$, $\theta(0) = \pi/3$, $\theta'(0) = 0$

matches ε (see Figure 10). However, the motion is not oscillatory. If the bead were to start at Ω_2 , $\theta'(\Omega_2) = 0$, however, $\theta''(\Omega_2) < 0$, as $\Omega_2 > \Omega_1$. As a result, θ' becomes negative and hence θ decreases towards Ω_1 . At Ω_1 , $\theta'' = 0$, whereas θ' has maximum magnitude but is still negative.

$$|\theta'_{max}| = |\theta'_{\theta=\Omega_1}| = \sqrt{k} - \frac{1}{\sqrt{k}} \quad (24)$$

Therefore θ continues to decrease towards zero. At $\theta = 0$, $\theta' = 0$ and θ'' is zero as well. Depending on its initial position, the bead will eventually reach $\theta = 0$, either directly, or after turning at $\pm\Omega_2$, with ever decreasing speeds. Once at this position, the bead will remain there until perturbed. The period of oscillation of the bead may be computed by direct integration as was done for the case of $0 \leq k < 1$ with $\varepsilon = 1$. However, by invoking the time reversal symmetry of the system, one can show that the bead will take an infinite amount of time to reach $\theta = 0$. Let us start with the premise that the bead reaches $\theta = 0$ after a finite time τ_1 . At τ_1 , $\theta' = 0$, and we may equally say that at $\tau = \tau_1$, the direction of θ' has been reversed. Due to time reversal symmetry, the bead must then retrace its path. Having reached $\theta = 0$ however, the bead must stay there forever, as θ' and θ'' are both zero at this position. Hence the bead cannot reach $\theta = 0$ in finite time.

(iv) $-1 < \varepsilon < 1$:

The bead oscillates between $\theta = \pm\Lambda$ corresponding to the turning points D and D' in Figure 10, where θ' is zero. Here, the bead has enough energy to overcome the local maxima at 0 and cross over to the other side. In a single period of oscillation, $|\theta'|$ attains its maximum value four times, as the bead crosses both the minima Ω_1 and $-\Omega_1$ in each half oscillation.

The time period can be calculated as,

$$T = 4 \int_0^\Lambda \frac{d\theta}{\sqrt{(\cos \theta - \cos \Lambda)(2 - k(\cos \theta + \cos \Lambda))}} \quad (25)$$

(v) $\varepsilon = 1$:

Both θ' and θ'' are zero at $\theta = \pm\pi$. Hence, if the bead were at an initial position $-\pi < \theta < \pi$, it will eventually reach $\pm\pi$ at ever decreasing speeds. The speed, $|\theta'|$ will be maximum at $\pm\Omega_1$ and will have a local minimum at $\theta = 0$.

(vi) $\varepsilon > 1$:

θ' is never zero as ε is greater than $U(\theta)$ for all θ . Thus θ increases or decreases indefinitely, depending on the sign of θ' . The bead will whirl around the entire hoop, in the same direction, past its initial position, periodically. The speed of the bead will increase and decrease periodically, with a local minimum at $\theta = 0$, global minimum at $\pm\pi$ and maximum at $\pm\Omega_1$. The trajectory will be similar to the ones shown in Figure 7.

IV. ENERGY AND CONSTRAINT FORCES

From (1) the total energy of the bead is,

$$E = \frac{1}{2}ma^2 \left[\dot{\theta}^2 + \omega^2 \sin^2 \theta - \frac{2g}{a} \cos \theta \right]. \quad (26)$$

Recalling the expression for the first integral of motion in (7), we may write,

$$E = mga \cdot \varepsilon + ma^2\omega^2 \sin^2 \theta. \quad (27)$$

The rate of change of energy is given by,

$$\frac{dE}{dt} = ma^2\omega^2 \dot{\theta} \sin 2\theta, \quad (28)$$

E is an even function of θ . This implies that the net change in energy over a path that takes the bead from θ to $-\theta$ or back to θ , is zero, although $\dot{\theta}$ may not be zero along the path. This accounts for the different oscillatory motions of the bead about 0 described in section III.

The constraint forces exerted by the hoop may be calculated using the method of Lagrange's undetermined multipliers. Introducing two Lagrange multipliers, λ and μ , the

Lagrangian of the system may be written as,

$$L = \frac{m}{2} [\dot{r}^2 + r^2(\dot{\theta}^2 + \sin^2 \theta \dot{\phi}^2)] + mgr \cos \theta + \lambda(r - a) + \mu(\phi - \omega t) , \quad (29)$$

with the constraint equations

$$r = a \quad \text{and} \quad \phi = \omega t . \quad (30)$$

Using the Euler-Lagrange equation, the equations of motion for r, ϕ and θ are,

$$\begin{aligned} \ddot{r} &= r[\dot{\theta}^2 + \dot{\phi}^2 \sin^2 \theta] + \frac{\lambda}{m} + g \cos \theta , \\ \frac{d}{dt}(mr^2 \dot{\phi} \sin^2 \theta) &= \mu , \\ \frac{d}{dt}(r^2 \dot{\theta}) &= r^2 \dot{\phi}^2 \sin \theta \cos \theta - gr \sin \theta . \end{aligned}$$

Substitution of the constraint equations in the above yield,

$$\begin{aligned} \lambda &= -ma[\dot{\theta}^2 + \omega^2 \sin^2 \theta] - mg \cos \theta , \\ \mu &= ma^2 \omega \dot{\theta} \sin 2\theta . \end{aligned}$$

λ and μ are the constraint force and torque along the radial and azimuthal directions respectively¹. As the hoop is assumed to be frictionless, it can only exert forces in a plane perpendicular to it. Hence, the θ component of the constraint force must be zero. This can be verified by the Newtonian approach. Let F_θ denote the constraint force along the $\hat{\theta}$ direction. Balancing the forces along $\hat{\theta}$ direction we get

$$\begin{aligned} F_\theta - mg \sin \theta &= ma(\ddot{\theta} - \omega^2 \sin \theta \cos \theta) , \text{ or,} \\ F_\theta &= ma[\ddot{\theta} + \frac{g}{a} \sin \theta - \omega^2 \sin \theta \cos \theta] . \end{aligned}$$

The factor within the brackets is zero as per (3), hence $F_\theta = 0$.

Therefore, the rate of work done by the constraint forces is,

$$P = F_\phi(a \omega \sin \theta) = \mu \omega = ma^2 \omega^2 \dot{\theta} \sin 2\theta . \quad (31)$$

which is equal to the rate of change of energy of the bead.

V. PHASE PORTRAITS AND BIFURCATIONS

We now study the nature of fixed points and bifurcations, and portray the phase space trajectories of the bead-hoop system. By defining a new variable $\theta_1 = \theta'$, (4) may be

transformed to a set of two first order equations as,

$$\theta' = \theta_1, \quad \text{and} \quad \theta'_1 = -\sin \theta(1 - k \cos \theta). \quad (32)$$

The system described by (4) is conservative as there exists a first integral of motion which was computed in section II. This conserved quantity represents an energy surface in the phase plane. The system motion takes place on this surface at constant height. That is, the effective energy remains a constant on the trajectories of the system. Therefore, any isolated minimum or maximum of this energy surface is a center and there cannot be any attracting fixed points or limit cycles³. The system is also reversible, as under the transformations,

$$(i) t \rightarrow -t, \quad \theta \rightarrow -\theta, \quad \text{and} \quad (ii) t \rightarrow -t, \quad \theta_1 \rightarrow -\theta_1 \quad (33)$$

the governing equations (32) remain invariant. This means that if $(\theta(t), \theta_1(t))$ is a solution, so are $(-\theta(-t), \theta_1(-t))$ and $(\theta(-t), -\theta_1(-t))$. The reversibility of the system does not admit any repelling fixed points. This can be argued as follows. Let us assume that a repelling fixed point does exist. If this is not at the origin, then by virtue of reversibility of the system, there must exist an attracting fixed point, located at the reflection of the repelling fixed point about θ or θ_1 axis. This however, is not possible as the system is conservative.

Were the origin to be a repeller, then trajectories infinitesimally close to the origin will move away from it in all directions. Reversibility requires that for every outward bound trajectory close to the origin in the first quadrant, there exists a trajectory moving towards the origin in the fourth quadrant. This is in contradiction to the assumption that the origin is a repeller. Hence, the fixed points of the bead-hoop system are either centers or saddles.

Equations (32) show that for all values of k , the fixed points lie on the θ axis, and in the first quadrant, all trajectories move right, as $\theta' > 0$.

When $0 \leq k \leq 1$, there are two fixed points for $\theta \in [0, \pi]$. When $k > 1$, an additional fixed point appears at $\theta = \cos^{-1}(1/k)$. We first investigate the fixed points and their nature by linear stability analysis. The effect of nonlinear terms is considered subsequently. A general form of (32) may be written as,

$$\theta' = f(\theta, \theta_1), \quad \theta'_1 = g(\theta, \theta_1).$$

A Taylor expansion about a fixed point (θ^*, θ_1^*) yields,

$$\xi' = f(\theta^*, \theta_1^*) + \xi \frac{\partial f}{\partial \theta} \Big|_{\theta^*, \theta_1^*} + \eta \frac{\partial f}{\partial \theta_1} \Big|_{\theta^*, \theta_1^*} + O(\xi^2, \eta^2, \xi\eta) + \dots \quad (34)$$

$$\eta' = g(\theta^*, \theta_1^*) + \xi \frac{\partial g}{\partial \theta} \Big|_{\theta^*, \theta_1^*} + \eta \frac{\partial g}{\partial \theta_1} \Big|_{\theta^*, \theta_1^*} + O(\xi^2, \eta^2, \xi\eta) + \dots \quad (35)$$

where, $\xi = \theta - \theta^*$ and $\eta = \theta_1 - \theta_1^*$. For small perturbations about the fixed point (θ^*, θ_1^*) , quadratic and higher terms in ξ and η may be neglected. The equations governing ξ and η are given by,

$$\begin{pmatrix} \xi' \\ \eta' \end{pmatrix} = \begin{pmatrix} \frac{\partial f}{\partial \theta} & \frac{\partial f}{\partial \theta_1} \\ \frac{\partial g}{\partial \theta} & \frac{\partial g}{\partial \theta_1} \end{pmatrix}_{\theta^*, \theta_1^*} . \quad (36)$$

The matrix on the rhs is the Jacobian matrix at the fixed point (θ^*, θ_1^*) .

The Jacobian matrix at the fixed point $(0, 0)$ is,

$$\mathbf{J}(0) = \begin{pmatrix} 0 & 1 \\ k-1 & 0 \end{pmatrix} . \quad (37)$$

As $k-1 < 0$, the eigenvalues $\lambda = \pm i\sqrt{1-k}$ are purely imaginary. Thus $(0, 0)$ is a linear center with angular frequency of revolution given by $\omega \approx \sqrt{1-k}$. On expanding ε in the neighbourhood of the origin,

$$2\varepsilon = \theta_1^2 + (1-k)\theta^2 - 1 + O(\theta^4) , \quad (38)$$

it is clear that $(0, 0)$ is a minimum of the effective energy. We therefore conclude that $(0, 0)$ is a non-linear center as well.

Thus, the trajectories close to the origin are elliptical with eccentricity $e = \sqrt{k}$. The trajectories start as circles when $k = 0$, and become elongated in the θ direction as k increases. For $(\pi, 0)$, the Jacobian matrix is,

$$\mathbf{J}(\pi) = \begin{pmatrix} 0 & 1 \\ k+1 & 0 \end{pmatrix} . \quad (39)$$

The eigenvalues of this matrix are real with opposite signs, $\lambda = \pm\sqrt{k+1}$. Hence, $(\pi, 0)$ is a saddle with eigenvectors given by, $\mathbf{v} = (1 \ \lambda)^T$. Therefore, $(1 \ \sqrt{k+1})^T$ is the unstable manifold with $\lambda = \sqrt{k+1}$ and $(1 \ -\sqrt{k+1})^T$ is the stable manifold with $\lambda = -\sqrt{k+1}$. They have equal and opposite slopes, whose value increases from 1 to $\sqrt{2}$ as k increases from 0 to 1.

The phase trajectories for $k = 0.75$ and $k = 1.0$ are shown in Figure 14. One can identify heteroclinic orbit or saddle connection, which is a trajectory connecting two saddles. A trajectory starting infinitesimally close to $\theta = -\pi$ with $\theta_1 = 0$, crosses the θ_1 axis at $\sqrt{2(\varepsilon + 1)}$. By reversibility, this trajectory must reach $\theta = \pi$, thus forming a heteroclinic orbit. It may be noted here that $\theta = \pi$ and $\theta = -\pi$ correspond to the same position on the hoop. The $\theta_1 - \theta$ plane is like the curved surface of a cylinder, with the $-\pi$ and π edges joined. The heteroclinic orbits in Figure 14 are thus homoclinic orbits on the cylinder starting and ending on the saddle at $(\pi, 0)$. The closed orbits around the center at origin

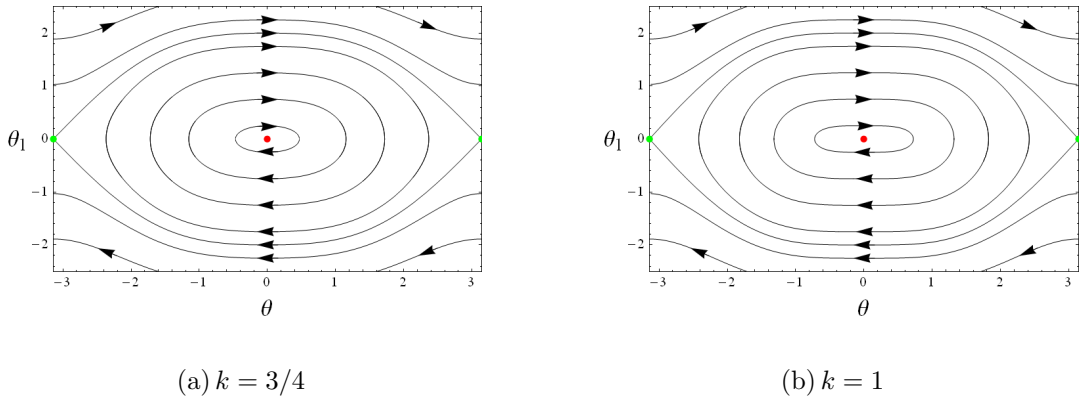


FIG. 14. Phase portraits for different k values

represent periodic oscillations about $\theta = 0$, for $-1 < \varepsilon < 1$, traditionally called librations. The saddle connection or heteroclinic orbit represents the delicate motion of the bead where it starts near the top of the hoop, swings past the bottom of the hoop and slows to a halt as it approaches the top of the hoop again. The trajectories above the saddle connection correspond to the whirling motion or complete revolution of the bead around the hoop.

When $k = 1$, the Jacobian at $(0, 0)$ becomes,

$$\mathbf{J}(0) = \begin{pmatrix} 0 & 1 \\ 0 & 0 \end{pmatrix}. \quad (40)$$

Consequently, both the eigenvalues vanish. This does not give us much information, so we expand the effective energy, ε , in the neighbourhood of the origin,

$$\varepsilon = \frac{\theta_1^2}{2} + \frac{\theta^4}{8} - 1 + O(\theta^6). \quad (41)$$

The point $(0, 0)$ remains a minimum of the energy surface and hence is still a center, though very weak. The weakness of the center is brought out by the elongated shape of the orbits in the phase plane (Figure 14). Close to $\theta = 0$, the decay of θ is very slow. This lethargic decay is termed ‘critical slowing down’ and sometimes signifies the onset of bifurcation³.

When $k > 1$, a new fixed point appears at $(\Omega_1, 0)$. As we noted in section III, the minima of $U(\theta)$ and hence the minima of the energy surface occur at $\pm\Omega_1$. Hence from our previous reasoning, $(\Omega_1, 0)$ is a center. This can be further verified by forming the Jacobian at $(\Omega_1, 0)$,

$$\mathbf{J}(\Omega_1) = \begin{pmatrix} 0 & 1 \\ -(k - 1/k) & 0 \end{pmatrix}. \quad (42)$$

$\mathbf{J}(\Omega_1)$ has purely imaginary eigenvalues $\lambda = \pm i\sqrt{k - 1/k}$. Thus, $(\Omega_1, 0)$ is a center, with angular frequency of libration $\omega \approx \sqrt{k - 1/k}$. Let $k = 1 + \delta$. Then $(1 + \delta)^{-1} = \cos \Omega_1$. Expanding both sides for small δ and equating the dominant terms, one finds that $\Omega_1 \sim O(\sqrt{\delta})$. Thus, Ω_1 increases much more rapidly than δ does.

On the other hand, at $(0, 0)$,

$$\mathbf{J}(0) = \begin{pmatrix} 0 & 1 \\ k - 1 & 0 \end{pmatrix} \quad (43)$$

now has real eigenvalues $\lambda = \pm\sqrt{k - 1}$. Therefore, the origin has transformed into a saddle having $(1 \ \sqrt{k - 1})^T$ as the unstable manifold and $(1 \ -\sqrt{k - 1})^T$ as the stable manifold. They become steeper as k increases. The fixed point at $(\pi, 0)$ continues to be a saddle as before.

A trajectory starting at $\theta \rightarrow 0^+$ and $\theta_1 = 0$ cuts the θ axes exactly at $\theta = \Omega_2$. By reversibility, we conclude that this forms a homoclinic orbit, enclosing the center at $(\Omega_1, 0)$. The heteroclinic orbits remain as before. We get closed orbits in the region of the phase-plane bounded by the homoclinic and the heteroclinic orbits (Figure 15). By expanding the effective energy about $(\Omega_1, 0)$, we find that the orbits near the center are approximate ellipses described by,

$$\theta_1^2 + \left(k - \frac{1}{k}\right)(\theta - \Omega_1)^2 = 2\varepsilon + \left(k - \frac{1}{k}\right) + O((\theta - \Omega_1)^3) \quad (44)$$

with eccentricity $e \approx \sqrt{|k - 1/k - 1|}$. These features are shown in the phase portraits in Figure 15. The physical interpretation of the trajectories is as follows : the fixed point $(\Omega_1, 0)$

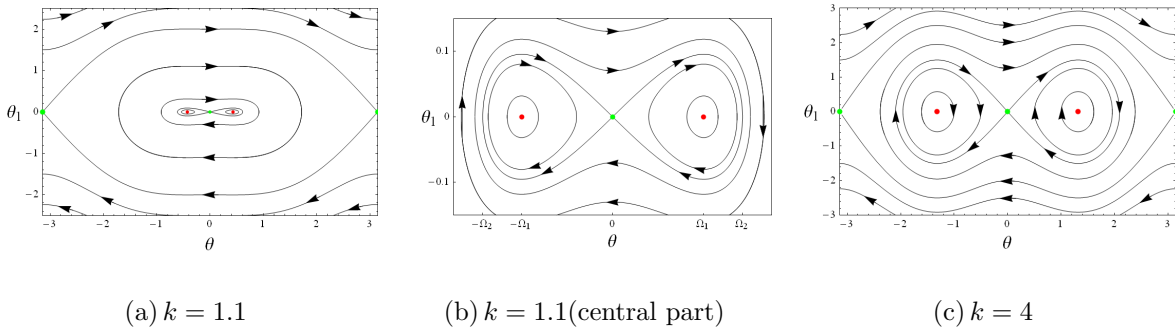


FIG. 15. Phase portraits for $k > 1$ showing homoclinic orbits.

is the stable equilibrium position. The small orbits around it represent periodic oscillations or librations. One can identify homoclinic orbits which begin and end at the same fixed point, the saddle at $(0, 0)$. This corresponds to the motion of the bead where it slows to a halt at $\theta = 0$. The closed orbits surrounding these correspond to oscillations about $\theta = 0$ with amplitude greater than Ω_2 of Figure 10 in section III. The heteroclinic orbits indicate the delicate motion where the bead slows to a halt at the top of the hoop. The trajectories outside it represent periodic whirling or complete revolutions of the bead around the hoop. These inferences are consistent with the motion of the bead as discussed in section III using graphical and differential equation analysis.

A change in the number and nature of fixed points of a dynamical system, as one of its parameters is varied is called bifurcation. When $k > 1$, the fixed point at $(0, 0)$ changes from a center to a saddle. Two new centers emerge on both sides of $(0, 0)$ at $\pm \cos^{-1}(1/k)$, moving away from the origin as k increases further. Therefore, the system undergoes a supercritical pitchfork bifurcation at the origin as k is varied through 1³. Also, $|\mathbf{J}(0)| = 0$ for $k = 1$. So, it can be called a zero eigenvalue bifurcation. It is also referred to as a symmetry-breaking bifurcation. The bifurcation diagram in Figure 16, encompasses both positive and negative values of k . For the bead-hoop system that we have studied, negative values of k have no physical meaning. However, there are systems with governing equations similar to (32), where negative values of k are allowed. For example, a charged particle moving on a vertically rotating circular wire, with a uniform magnetic field B_0 in the downward vertical direction, has the same governing equations as (32), but with the parameter k given by,

$$k = \frac{\omega^2}{(g/a)} - \frac{qa\omega B_0}{mg} \quad (45)$$

This allows negative values of $k \geq -\omega_L^2/\omega_c^2$, where ω_L is the Larmor frequency. For this

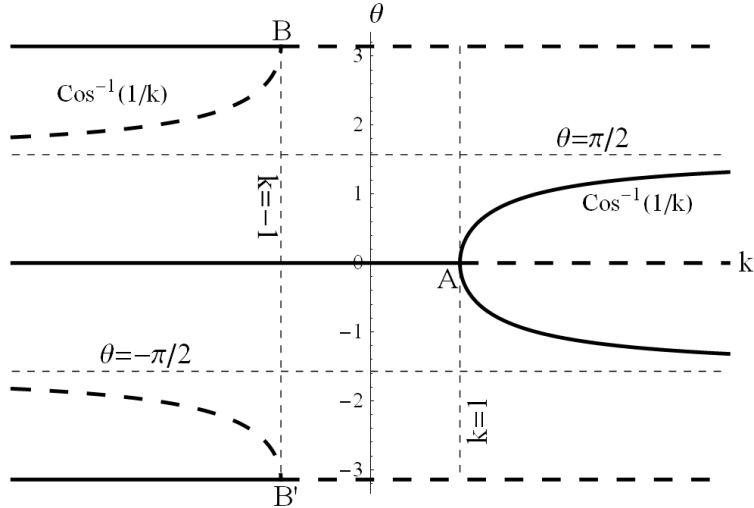


FIG. 16. The bifurcation diagram for both positive and negative k . Pitchfork bifurcation takes place at A and B . B and B' represent the same point.

system, negative k values become relevant. In Figure 16, the solid lines denote center and the dashed lines denote saddle. As k is made more negative than -1 , $(\pm\pi, 0)$ changes from a saddle to a center and two symmetrical saddle points fork out towards $\theta = \pm \cos^{-1}(1/k)$ (pitchfork / symmetry-breaking bifurcation). If we imagine the diagram to be on a cylindrical surface with the top and bottom borders joined end to end, then the figure is very symmetrical (Figure 16).

VI. CONNECTIONS WITH OTHER SYSTEMS

The system we have studied has interesting connections and similarities with a variety of other physical systems. As mentioned previously, the same set of equations are obtained for a charged particle moving on a vertically rotating circular wire, in the presence of a uniform magnetic field directed vertically downward. However, the parameter k can take negative values as well. The phase portraits, nature of fixed points and bifurcations can thus be analyzed in a similar manner.

The system exhibits spontaneous symmetry breaking at $k = 1$ ($\omega = \omega_c$), quite similar to a Landau second-order phase transition⁴⁻⁷. The critical angular velocity of the hoop, ω_c , is analogous to the critical temperature T_c and the equilibrium position of the bead to the order parameter in a Landau system.

Another example is the Duffing oscillator described by the equation,

$$\ddot{x} + x + \epsilon x^3 = 0 . \quad (46)$$

Expanding (4), for $0 \leq k \leq 1$, in the neighbourhood of $\theta = 0$ we get,

$$\theta'' + (1 - k)\theta + \left(\frac{2k}{3} - \frac{1}{6}\right)\theta^3 = O(\theta^5) . \quad (47)$$

If we define $u = \sqrt{1 - k}\tau$, then the above equation may be written as,

$$\frac{d^2\theta}{du^2} + \theta + \frac{4k - 1}{6(1 - k)}\theta^3 = O(\theta^5) , \quad \text{for } 0 \leq k < 1. \quad (48)$$

Neglecting terms of order 5 and higher in θ , the equation reduces to the Duffing oscillator equation (46). Thus the nature of fixed points and bifurcations studied for the bead-hoop system in the small amplitude limit, with $0 \leq k < 1$, hold for the Duffing oscillator as well. The Duffing equation (46) describes the undamped motion of a unit mass attached to a nonlinear spring with restoring force $F(x) = -x - \epsilon x^2$. The Duffing equation is also a conservative system. The coefficient ϵ , of the nonlinear term is related to the parameter k of the bead-hoop system as $\epsilon = (4k - 1)/(6(1 - k))$. As k is varied from 0 to 1, ϵ increases from $-1/6$ to ∞ . For this range of ϵ , the Duffing oscillator does indeed have a nonlinear center at the origin³.

A variation of our system is the hoop rotating about a horizontal axis. This system can operate as a one-dimensional ponderomotive particle trap⁸.

The rigid pendulum can be considered a special case of our system with $k = 0$, and many problems in various branches of physics, such as, the theory of solitons, the problem of superradiation in quantum optics, and Josephson effects in weak superconductivity can be reduced to the differential equation describing the motion of a pendulum⁹.

Let us now discuss briefly the case when the hoop is not maintained at constant rotation, i.e., $\dot{\phi}$ is not a constant. Initially, the hoop is given some non-zero $\dot{\phi}$ and the bead-hoop system is left to itself. The total energy of the system is conserved, but both $\dot{\theta}$ and $\dot{\phi}$ vary with time. From the Lagrangian of the system, one can arrive at the following,

$$\dot{\phi} = \frac{k_1}{M + m \sin^2 \theta} , \quad (49)$$

$$\theta'' = -\sin \theta \left[1 - \frac{a_1 \cos \theta}{(1 + b \sin^2 \theta)^2} \right] , \quad (50)$$

where M and m denote the masses of the hoop and the bead respectively, and $a_1 = k_1^2 a / (M^2 g)$, $b = m/M$. When $b \ll 1$, i.e., $m \ll M$, $\dot{\phi} \approx \frac{k_1}{M} = \omega$, a constant. In this limit, the hoop has very large inertia compared to the bead, and therefore a high tendency to resist any change in its energy.

$$a_1 = \left(\frac{k_1}{M} \right)^2 \frac{a}{g} = \frac{\omega^2}{\omega_c^2},$$

Hence, $\theta'' = -\sin \theta \left(1 - \frac{\omega^2 a}{g} \cos \theta \right)$.

which is the same as (4).

CONCLUSION

The diverse modes of motion of a bead moving without friction, on a vertically rotating circular hoop have been explored using a simple theoretic approach based on symmetry arguments and elementary calculus. This simple system exhibits several features of nonlinear dynamics and hence this study can serve as a good background for investigating more complicated nonlinear systems.

REFERENCES

- ¹ Goldstein H 1980-07 *Classical Mechanics* (Addison-Wesley, Cambridge, MA)
- ² Jordan D W and Smith P 1999 *Nonlinear Ordinary Differential Equations : An Introduction to Dynamical Systems* (Oxford University Press, New York)
- ³ Strogatz S 2001 *Nonlinear Dynamics And Chaos: Applications To Physics, Biology, Chemistry, And Engineering* (Addison-Wesley, Reading, MA)
- ⁴ Sivardière J 1983 A simple mechanical model exhibiting a spontaneous symmetry breaking *Am. J. Phys.* **51** 1016.
- ⁵ Landau L and Lifschitz E M 1959 *Statistical Physics* (Pergamon, London)
- ⁶ Fletcher G 1997 A mechanical analogue of first- and second-order phase transitions *Am. J. Phys.* **65** 74.

- ⁷ Mancuso Richard V 1999 A working mechanical model for first- and second-order phase transitions and the cusp catastrophe *Am. J. Phys.* **68** 271.
- ⁸ Johnson A K and Rabchuk J A 2009 A bead on a hoop rotating about a horizontal axis : A one-dimensional ponderomotive trap *Am. J. Phys.* **77** 1039
- ⁹ Butikov E I 1999 The rigid pendulum -an antique but evergreen physical model *Eur. J. Phys.* **20** 429